BRAIN CONNECTIVITY
Volume 4, Number 3, 2014

DOI: 10.1089/brain.2013.0160

Combining Spatial Independent Component Analysis with Regression to Identify the Subcortical Components of Resting-State fMRI Functional Networks

Caroline Malherbe,[1,2] Arnaud Messé,[1,2] Eric Bardinet,[2–4] Mélanie Pélégrini-Issac,[1,2] Vincent Perlbarg,[1,2] Guillaume Marrelec,[1,2] Yulia Worbe,[2,3,5] Jérôme Yelnik,[3,5] Stéphane Lehéricy,[2–4] and Habib Benali[1,2]

Abstract

Functional brain networks are sets of cortical, subcortical, and cerebellar regions whose neuronal activities are synchronous over multiple time scales. Spatial independent component analysis (sICA) is a widespread approach that is used to identify functional networks in the human brain from functional magnetic resonance imaging (fMRI) resting-state data, and there is now a general agreement regarding the cortical regions involved in each network. It is well known that these cortical regions are preferentially connected with specific subcortical functional territories; however, subcortical components (SC) have not been observed whether in a robust or in a reproducible manner using sICA. This article presents a new method to analyze resting-state fMRI data that enables robust and reproducible association of subcortical regions with well-known patterns of cortical regions. The approach relies on the hypothesis that the time course in subcortical regions is similar to that in cortical regions belonging to the same network. First, sICA followed by hierarchical clustering is performed on cortical time series to extract group functional cortical networks. Second, these networks are complemented with related subcortical areas based on the similarity of their time courses, using an individual general linear model and a random-effect group analysis. Two independent resting-state fMRI datasets were processed, and the SC of both datasets overlapped by 69% to 99% depending on the network, showing the reproducibility and the robustness of our approach. The relationship between SC and functional cortical networks was consistent with functional territories (sensorimotor, associative, and limbic) from an immunohistochemical atlas of the basal ganglia.

Key words: brain networks; fMRI; regression; resting-state; spatial independent component analysis; subcortex

Introduction

Functional brain networks are defined as sets of gray matter regions showing synchronous neuronal activities (Varela et al., 2001). Low-frequency fluctuations in the blood-oxygen-level dependent (BOLD) signal (0.01–0.1 Hz) during resting-state functional magnetic resonance imaging (fMRI) should reflect intrinsic neuronal activity, which represents the condition of the human brain in the absence of external stimuli (Biswal et al., 1995; Fox and Raichle, 2007). Regions with similar low frequency fluctuations correspond to relevant functional networks reflecting cognitive, emotional, and sensorimotor processes (Damoiseaux et al., 2006; Smith et al., 2009).

Numerous reports in monkeys using biological tracers that diffuse through antero- or retrograde axonal transport have demonstrated the presence of cortico-subcortical loops (Parent et al., 2000; Smith et al., 2004), which connect cortical regions to specific subcortical regions and are recognized as being crucial to functions such as motor skills or cognition (Alexander et al., 1986; Purves et al., 2004). Zhang and colleagues (2008) used resting-state fMRI in humans and an approach based on regions of interest and partial correlation to study functional connectivity between thalamic nuclei and specific cortical regions. Similarly, using regions of interest to analyze functional connectivity between the striatum and cortical regions, Gopinath and coworkers

[1]Inserm/UPMC Univ Paris 6, UMR-S 678, Laboratoire d'Imagerie Fonctionnelle, Paris, France.
[2]Univ Paris 11, IFR 49, DSV/I2BM Neurospin, Gif-sur-Yvette, France.
[3]Inserm/UPMC Univ Paris 6, UMR-S 975, CNRS, UMR 7225, Centre de Recherche de l'Institut du Cerveau et de la Moelle épinière, Paris, France.
[4]Groupe Hospitalier Pitié-Salpêtrière, CENIR—Centre de NeuroImagerie de Recherche, Paris, France.
[5]Assistance Publique-Hôpitaux de Paris, Groupe Hospitalier Pitié-Salpêtrière, Centre d'Investigation Clinique Inserm CIC 9503, Pôle des Maladies du Système Nerveux, Paris, France.

(2011) demonstrated that the striatum had strong functional links with sensorimotor and attentional networks as well as with emotional networks.

Resting-state fMRI networks have also been explored using data-driven approaches where the brain is analyzed in its entirety without any a priori information (Beckmann et al., 2005; Perlbarg et al., 2008). Habas and associates (2009) extracted subcortical regions associated with cortical and cerebellar regions by using a group spatial independent component analysis (sICA), albeit only on a limited number of functional networks (the default mode, executive control, and salient networks). However, they did not conduct any reproducibility study on the results. In previous articles (Damoiseaux et al., 2006; Perlbarg et al., 2008; Smith et al., 2009), the authors differentiated functional networks by the presence or absence of specific cortical regions. Subcortical regions (when present) were only listed and not actually taken into consideration in the classification of functional networks. Most of the time, sICA found the striatum and the thalamus gathered in a few number of components (Damoiseaux et al., 2008; Kim et al., 2013; Robinson et al., 2009) and was not able to subdivide these regions into subcortical structures associated with patterns of cortical areas.

Thus, sICA as it is usually conducted, that is, on the whole brain, mostly gives access to a set of cortical networks with scarce subcortical components (SC) and does not actually identify cortico-subcortical networks. Intuitively, this suggests that subcortical and cortical regions should be considered separately through distinct analyses and that a functional hypothesis is needed to further ensure a correct association between subcortical and cortical regions belonging to the same functional network. In this work, we assume that the time courses (i.e., the variation of acquired BOLD signals over time) in the striatum and the thalamus are similar to those in associated cortical components.

The objective of this work is to propose a robust and reproducible approach to identify the SC of functional networks from resting-state fMRI data. We first describe the method: On the one hand, sICA is carried out for cortical regions only, which yields functional cortical networks. On the other hand, SC are identified by means of a general linear model (GLM) applied to the striatum and the thalamus, based on the hypothesis that the time course in these regions should covary with that of cortical components belonging to the same network. The resulting SC are validated by a comparison with an immunohistochemical functional atlas (Bardinet et al., 2009; Yelnik et al., 2007), which provides a specific labeling of subcortical functional territories (SFT). Then, reproducibility is assessed using an additional dataset. Lastly, limitations and perspectives are discussed in view of the existing literature.

Methods

The proposed method consisted of several steps. First, the striatum and the thalamus were masked out and sICA combined with a hierarchical procedure was carried out on cortical data, extracting group and corresponding individual spatial components. We then linked the cortical components to regions in the striatum and the thalamus based on time course similarity, using a GLM. The procedure yielded a parametric map of SC associated with each cortical component. These cortical and subcortical regions, once associated, finally defined cortico-subcortical functional networks. Figure 1 shows a flowchart of the procedure.

Identification of functional cortical networks

Let $\boldsymbol{Z}$ be the T-by-N matrix of data acquired at rest for each subject with N voxels and T time samples. Using an immunohistochemical postmortem atlas (Bardinet et al., 2009; Yelnik et al., 2007), we obtained a mask of the striatum and the thalamus in the native individual space. Using this mask, we partitioned $\boldsymbol{Z}$ into two datasets, $\boldsymbol{Z_C}$ and $\boldsymbol{Z_{SC}}$. Dataset $\boldsymbol{Z_{SC}}$ contained only data from subcortical (i.e., striatal and thalamic) regions, and complementary dataset $\boldsymbol{Z_C}$ contained data from the cortex, the white matter, and the cerebrospinal fluid (CSF). $\boldsymbol{Z_C}$ is a T-by-N_1 matrix and $\boldsymbol{Z_{SC}}$ is T-by-N_2, with N_1 and N_2 being the number of voxels.

The first step of the analysis consisted of extracting cortical networks from $\boldsymbol{Z_C}$ using group sICA as implemented in the network detection using ICA (NEDICA) software (Perlbarg et al., 2008). More specifically, the 40 spatial independent components (IC) that explained most variance were first extracted using sICA for each subject in his/her native space. From the sICA model, these IC are associated with time courses. The spatial IC obtained for all subjects were then normalized into the MNI standard space and clustered into classes that were representative of the population. To do so, a hierarchical clustering algorithm that maximized within-class spatial similarity (Hartigan, 1975) was used and yielded a similarity tree. Spatial similarity was quantified by a distance d derived from the spatial correlation corr(IC_i,IC_j) between two normalized IC, as follows:

$$d(\mathrm{IC}_i, \mathrm{IC}_j) = \sqrt{1 - \mathrm{corr}(\mathrm{IC}_i, \mathrm{IC}_j)}. \quad (1)$$

From the similarity tree, all IC were partitioned into classes that were the most representative of the population, using an *ad hoc* automatic procedure detailed in Appendix A. Note that a subject may not contribute to a class at all or contribute with one or several components. All normalized spatial maps in each class were then averaged, and the resulting average map was thresholded at $p < 0.05$ using t-test statistics (corrected for multiple comparisons by using the false discovery rate approach [Genovese et al., 2002]). Finally, thresholded average maps of all classes were visually inspected to select a number R of maps that exhibited a known spatial organization. These maps are further referred to as cortical networks. The remaining maps were related to noise processes (either physiological or physical).

Identification of SC

The second step consisted of assigning each voxel in the striatum and the thalamus to one cortical network, based on the hypothesis that the time course of subcortical voxels should covary with that of cortical components belonging to the same network. For each subject in his/her native space, we first regressed the signal within each subcortical voxel on the R characteristic time courses of the cortical networks (Worsley et al., 2002)

$$\boldsymbol{Z}_{\mathrm{SC}} = \boldsymbol{AB} + \boldsymbol{\varepsilon}, \quad (2)$$

where $\boldsymbol{A} = (\mathbf{a}^r)_{r=1,\ldots,R}$ is the T-by-R matrix of the characteristic time courses, $\boldsymbol{B}$ is the R-by-N_2 matrix of regressors to be estimated, and $\boldsymbol{\varepsilon}$ is an independent and identically distributed

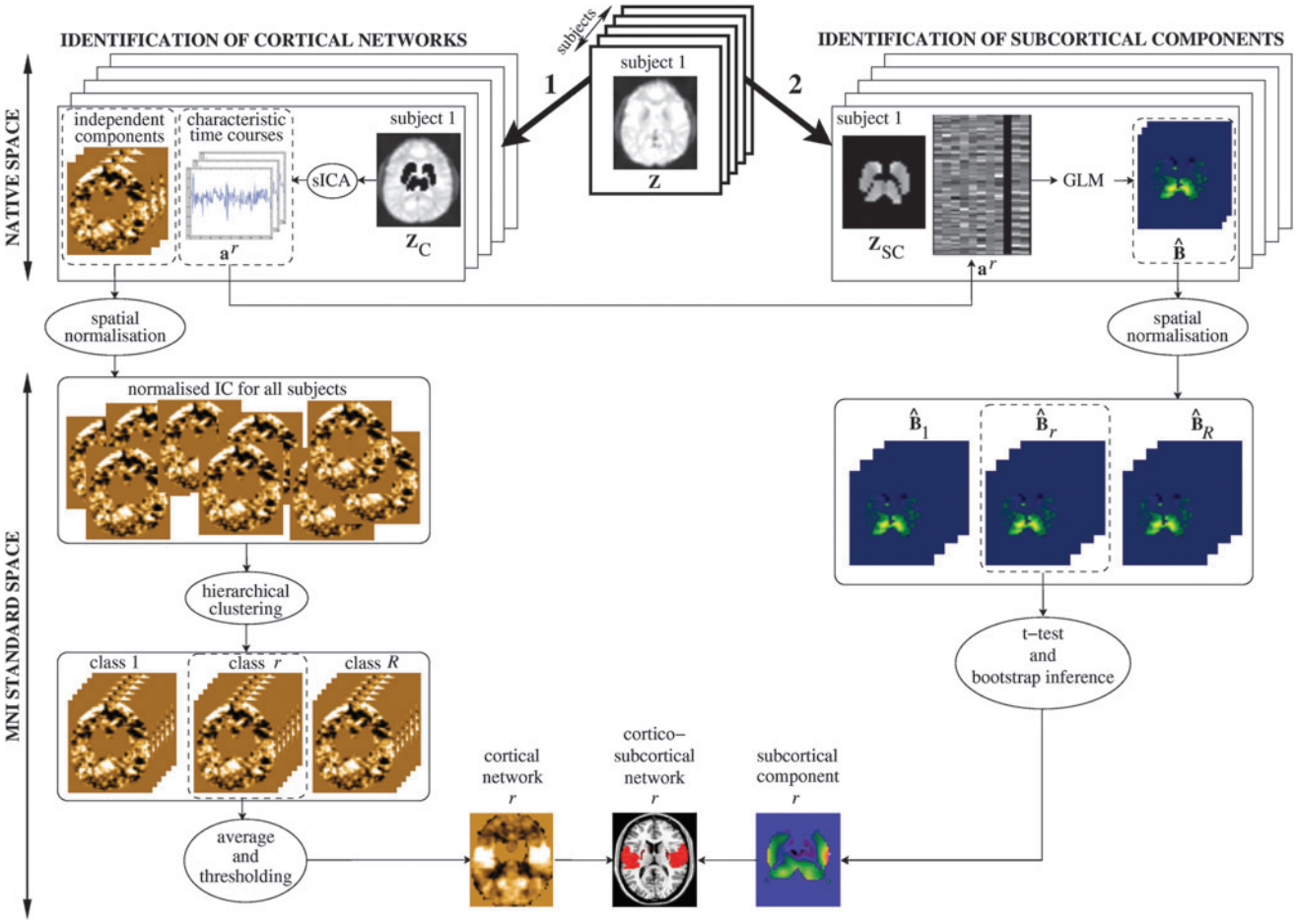

FIG. 1. Flowchart of the method. Individual analyses are conducted in the native space of each subject. Group analyses are conducted in the standard MNI space.

Gaussian noise. The characteristic time course of a cortical network was determined as follows. When only one component from the subject contributed to the construction of a network, the time course of this component as estimated from sICA (i.e., in the native space) was considered the characteristic time course for this network. When several components from the same subject contributed to the construction of a network, the average of their time courses was considered the characteristic time course. Conversely, if a subject did not contribute to the construction of a network, he/she was simply excluded from the subsequent analysis.

For each subject, this analysis provided one map $\hat{\boldsymbol{B}}_r$ of regression coefficients for each cortical network r. To put it differently, once all individual GLM were completed, we obtained a number S_r of regression coefficients maps for each cortical network, with S_r being the number of subjects contributing to this network. These maps contained subcortical voxels whose time course was correlated to the characteristic time course of the network. They were further spatially normalized to the MNI standard space.

For each network r, a parametric random-effect analysis was then performed and a voxelwise Student's t-test was carried out to test the null hypothesis that the average of the S_r maps was zero. This provided us with a t-value for each voxel, denoted by t_0. A nonparametric bootstrap approach was then used to ensure robust inference. More precisely, a set of 10,000 samples were created by resampling 10,000 times the S_r maps with replacement. For each sample, a new voxelwise t-value was computed, denoted by t^*. Final statistical inference was finally conducted based on the achieved significance level Q, defined as follows (Efron and Tibshirani, 1993):

$$Q = \frac{\text{card}(t^* \geq t_0)}{10,000}, \tag{3}$$

where card(A) denotes the cardinality of set A. As a result of this procedure, the group maps comprising subcortical voxels were reproducible across subjects. These maps are further referred to as SC.

Lastly, cortico-subcortical functional networks were obtained by combining the cortical group maps from NEDICA analysis and the associated SC obtained from GLM and bootstrap inference.

Validation

Cortical networks

Spatial and frequential comparisons were carried out in order to validate the functional cortical networks obtained

from $\mathbf{Z}_C$ data. Indeed, masking the striatum and the thalamus before NEDICA analysis naturally raises the following questions: Are there any differences between cortical spatial components, *depending on whether* fMRI data comprise the striatum and the thalamus or not? We, therefore, tested the influence of the presence of these subcortical structures on the extraction of cortical components with sICA at the individual level, and on the functional networks at the group level. To this end, cortical networks obtained from the complete data ($\mathbf{Z}$) were compared with those obtained from the data where subcortical voxels were masked ($\mathbf{Z}_C$).

To compare their spatial patterns, matching between group networks extracted from $\mathbf{Z}$ data and those extracted from $\mathbf{Z}_C$ data was carried out visually by an expert (J.Y.); similar networks were assigned the same label. The spatial overlap of group networks with the same label was then defined by the ratio: $N_{id}/(N_{id}+N_{diff})$, where N_{id} is the number of voxels identified with the same network label for both datasets and N_{diff} is the number of voxels with different labels.

To compare their temporal patterns, we resorted to frequency analysis. The power spectra of the signals from sICA components were compared as follows. First, the power spectrum for a given group network r was obtained by calculating the power spectra of all individual characteristic time courses [$\mathbf{a}^r$, see Eq. (2)] of the components contributing to this network and averaging these spectra. Then, we calculated the correlation, otherwise known as the ''match-correlation,'' between the power spectrum of each group network from $\mathbf{Z}_C$ data and that of the corresponding group network obtained from $\mathbf{Z}$ data.

To further quantify temporal similarity at the individual level, the correlation (with associated p-value) between the time course obtained from $\mathbf{Z}$ for each subject and each network and that obtained from $\mathbf{Z}_C$ for the same subject and the same network (when it existed) was computed. For each network, we counted how many times this correlation was significant ($p<0.05$). Correlation values were finally averaged across subjects.

Subcortical components

In this section, we wished to validate the location of the subcortical regions corresponding to the different functional networks. More precisely, the purpose was to accurately classify which parts of the striatum and the thalamus were specific to a given functional network to assess whether the proposed functional segregation was consistent with a segmentation from an atlas. In order to do this, we used an immunohistochemical atlas (Bardinet et al., 2009; Yelnik et al., 2007), which describes the caudate nucleus, the putamen, and the thalamus, and their functional segmentation in sensorimotor, limbic, and associative territories. Each subcortical territory from the atlas is indexed according to its functional domain. For example, the putamen is divided into three different and disjoint structures: the associative, sensorimotor, and limbic putamen. These structures are referred to as SFT in the rest of this article. The right and left hemispheres are differentiated for each structure.

Specifically, for each functional network at the group level, the corresponding SC (i.e., thresholded group maps in the MNI standard space obtained from Identification of SC section) were mapped to the atlas with a specific procedure (Bardinet et al., 2009) so as to verify whether these components were parts of specific SFT. In order to quantify the overlap between the atlas and the SC, we computed

- the volume of the intersection between each atlas territory (SFT_j) and each subcortical component obtained for a network r and a threshold p (SC_r^p), denoted by

  $V(SFT_j \cap SC_r^p)$, where $V(.)$ is the volume in voxels;

- the relative importance of a functional territory within the subcortical component of a given network, defined as follows:

$$V_{comp} = V(SFT_j \cap SC_r^p)/V(SC_r^p). \quad (4)$$

Reproducibility

In this section, the aim was to assess the reproducibility of the method by applying the proposed approach to two different datasets. Only the subcortical group components were studied, as reproducibility of the cortical regions has been widely reported in the literature. We examined the overlap between thresholded SC ($p<0.01$, uncorrected) for both datasets and each cortical network. To do so, we calculated N_{id} as the number of voxels identified with the same network label for both datasets and N_{diff} as the number of voxels with different labels. The overlap was then defined as in Cortical Networks section by the ratio: $N_{id}/(N_{id}+N_{diff})$. Furthermore, differences in spatial distribution of the SC in atlas SFT (V_{comp}) between datasets were assessed using a two-sample nonparametric test that tests the equality of two distributions, the Kolmogorov–Smirnov (KS) test.

MRI Data

Dataset 1

Twenty healthy volunteers (right handed, age 24 – 30, 12 men) provided their informed consent and took part in a study comprising the acquisition of two resting-state fMRI sessions and a high-resolution anatomical image. The protocol was approved by the ethics committee of the Centre de Recherche de l'Institut Universitaire de Gériatrie de Montréal (CRIUGM; Montreal QC, Canada). Subjects lay down in the magnet and were asked to stay still, to keep their eyes closed, and to restrain from overt activity. Functional MRI series were recorded using a single-shot, gradient-recalled echo planar imaging sequence (field of view: $224\times224\,mm^2$; repetition time [TR]: 2500 msec; echo time [TE]: 30 ms, flip angle: 90°). One hundred and sixty volumes were acquired for each run, and each volume consisted of 41 contiguous axial slices (3.5 mm isotropic voxels). The anatomical volume (128 axial slices, voxel size: 1 mm isotropic) was acquired using a three-dimensional, spoiled gradient echo sequence (TR: 22 msec, TE: 4 msec, flip angle: 30°; matrix size: 256×256 voxels). All data were recorded using a 12-channel 3T Siemens TRIO magnet at the CRIUGM.

Dataset 2

We used a dataset kindly provided by A. Villringer and freely available from the 1000 Functional Connectomes

Project website (http://fcon_1000.projects.nitrc.org) (Biswal et al., 2010). The acquisitions were performed in Leipzig, Germany, on 37 healthy subjects (age 20 – 42, 16 men). Acquisition parameters available to us were as follows: for the resting-state fMRI data, 195 volumes of 34 contiguous axial slices, matrix size: 64×64 voxels, voxel size: $3 \times 3 \times 4$ mm, TR = 2300 msec; for the T_1-weighted anatomical volume, 256 axial slices, matrix size: 176×240 voxels, voxel size 1 mm isotropic.

Preprocessing of fMRI data

All preprocessing was performed using the SPM5 software (www.fil.ion.ac.uk/spm/software/spm5). Functional MRI data were corrected for slice-timing effects and subject's rigid motion and spatially smoothed with a 3D isotropic Gaussian kernel with a full width at a half maximum of 5 mm. Individual estimated motion parameters as well as mean signals of the white matter and of the CSF were included as confound regressors in the GLM that was used to identify SC (Identification of SC section). The mean white matter and CSF signals were computed in white matter and CSF masks obtained by segmenting the anatomical image of each subject during the normalization procedure (see Normalization Procedure section). This yielded white matter and CSF images representing the probabilities of finding white matter or CSF at any point. The final white matter and CSF masks were obtained by suppressing voxels with a probability less than 0.7.

Normalization procedure

When necessary for group analyses, the transformation from the individual space to the standard MNI space was computed as follows: Functional images were first coregistered to the structural T_1-weighted image of each subject; then, a nonlinear transformation was calculated to map the structural image to the SPM5 T_1-weighted template in the MNI space. This transformation was subsequently applied, on the one hand, to all individual cortical IC obtained from $\mathbf{Z}_C$ analysis (Identification of Functional Cortical Networks section) and, on the other hand, to the individual regression coefficient maps obtained in subcortical structures from $\mathbf{Z}_{SC}$ analysis (Identification of SC section).

Results

Results obtained for dataset 1

At the group level, NEDICA extracted 11 functional networks from $\mathbf{Z}$ data and 10 from $\mathbf{Z}_C$ data. For $\mathbf{Z}_C$, the variance explained by the 40 IC ranged from 57.2% to 82.2% of the total variance for all subjects and runs (mean: 68.6%). Similar values were obtained for dataset 2. Ten of the 11 networks obtained from $\mathbf{Z}$ were very similar to those obtained from $\mathbf{Z}_C$ and were consequently labeled identically according to the classification proposed by Smith and colleagues (2009). We obtained three networks related to attentional processes—a dorsal attentional network (dATT) as well as a left and a right ventral attentional network (LvATT and RvATT, respectively)—, a default mode network (DM), a limbic network (LIMB), a visual network (VIS), two motor networks—a premotor network (MOT) and a sensorimotor network (MOT2)—, a network related to executive control (EXCTR), and a salient network (SAL).

The only network extracted from $\mathbf{Z}$ that did not correspond with any of the networks extracted from $\mathbf{Z}_C$ mostly comprised the caudate nucleus, the putamen, and a large part of the thalamus, all bilaterally (Fig. 2). Quantification of the resemblance between networks extracted from $\mathbf{Z}$ and from $\mathbf{Z}_C$ (Table 1) showed a large overlap of networks with the same label. Table 1 further shows that the mean correlation between time courses of networks obtained from $\mathbf{Z}$ and $\mathbf{Z}_C$ was high and significant for most of the subjects. This highlights the fact that the networks extracted from the two datasets were very similar not only spatially but also temporally. Moreover, an analysis of the power spectra revealed that the match correlation was systematically greater than 0.95.

Figure 3 shows the MOT network obtained from $\mathbf{Z}$ and $\mathbf{Z}_C$. Both networks were spatially similar, but the parahippocampal gyrus was only present in the network extracted from $\mathbf{Z}$. Figure 4 shows all the cortico-subcortical networks were obtained with the proposed method from the first dataset. While the MOT network obtained from $\mathbf{Z}$ included only a few voxels in the putamen (Fig. 3), the method combining sICA and the GLM approach identified numerous voxels in the putamen (Fig. 4).

The comparison between SC obtained using the proposed method and functional territories from the atlas is illustrated in Figure 5, which shows for the MOT network the regions classified as sensorimotor, such as the sensorimotor putamen and the pulvinar in the thalamus.

Comparison of datasets 1 and 2

Figures 6 and 7 show V_{comp} (SC thresholded at $p < 0.01$, uncorrected) for the right and left hemispheres, respectively. In the first dataset, the most involved SFT were the right and left sensorimotor putamen for both motor networks (MOT

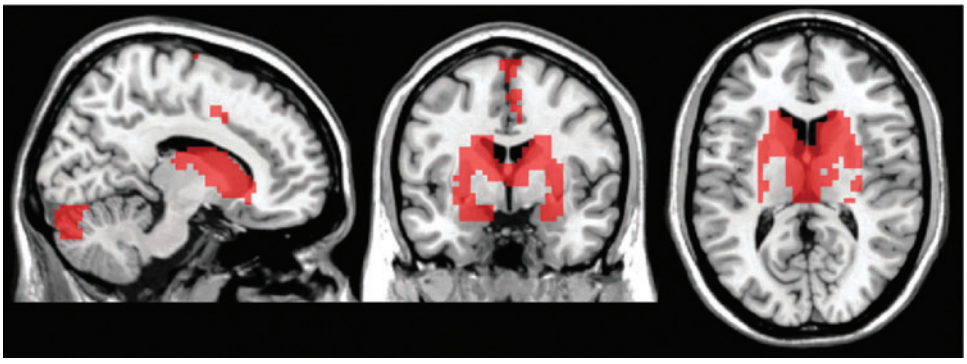

FIG. 2. Component obtained with NEDICA from $\mathbf{Z}$ data, comprising mostly subcortical structures. All images in the article are in radiological convention: The right hemisphere is on the left of the axial view.

Table 1. Comparison Between Cortical Regions of Networks with the Same Label Obtained from Z and from Z_C

Label	*Overlap (%)*	*Correlation*	$p < 0.05$
LvATT	0.9702	0.8346	19/20
RvATT	0.9702	0.8446	20/20
dATT	0.9749	0.7558	18/20
LIMB	0.9820	0.9240	20/20
EXCTR	0.9717	0.5430	16/20
SAL	0.9656	0.5952	20/20
MOT	0.9765	0.3315	15/20
MOT2	0.9630	0.8897	20/20
DM	0.9698	0.8730	19/20
VIS	0.9744	0.6929	19/20

First column: network label; second column: relative overlap of cortical regions for networks with the same label but obtained from Z and from Z_C; third column: mean correlation value across subjects between characteristic time courses obtained from Z and from Z_C; fourth column: proportion of subjects with $p < 0.05$ for the p-value associated to correlation.

dATT, dorsal attentional network; DM, default mode network; EXCTR, network relating to executive control; LIMB, limbic network; LvATT, left ventral attentional network; MOT, premotor network; MOT2, sensorimotor network; RvATT, right ventral attentional network; SAL, salient network; VIS, visual network.

and MOT2) and the associative putamen for the MOT2 network. For the default mode network, the main SFT were the associative and limbic caudate nucleus, the limbic putamen, as well as several (ventro-lateral and medio-dorsal) thalamic nuclei. A comparison of datasets 1 and 2 revealed greater stability of the results in the right hemisphere than in the left hemisphere.

Furthermore, no statistical difference was observed (KS tests, all nonsignificant) when comparing the spatial distributions of the LvATT, LIMB, dATT, EXCTR, SAL, DM, MOT, and MOT2 networks, bilaterally, confirming a very stable extraction of SC. Reproducibility for the RvATT network was less satisfactory for the left hemisphere only (KS test, $p < 0.05$).

Table 2 summarizes the overlap scores between datasets 1 and 2. Overlap scores were greater than 69% for all networks; more than 90% overlap was achieved for the DM network. This highlights the good consistency between the two datasets.

Discussion

In the past years, studies conducted on resting-state fMRI data have mainly reported functional networks on the basis of their cortical components (Damoiseaux et al., 2006; Perlbarg et al., 2008; Smith et al., 2009) and only a few studies extracted subcortical regions, either in a few number of components (Damoiseaux et al., 2008; Kim et al., 2013; Robinson et al., 2009) or associated to cerebellar and cortical regions (Habas et al., 2009).

In this article, we put forward a new method for extracting cortico-subcortical networks from resting-state fMRI data. First, using sICA at the individual level followed by a hierarchical classification at the group level, cortical networks were extracted from data where the striatum and the thalamus had been masked out. Then, SC associated to the cortical regions were extracted from the striatum and the thalamus data exclusively, by means of an individual GLM and statistical inference at the group level, using a bootstrap technique.

The proposed method better characterized cortico-subcortical functional loops than the NEDICA method alone. Damoiseaux and coworkers (2008) and Robinson and associates (2009) demonstrated that when extracting functional networks using sICA, they obtained a single component grouping together a large part of the pallidum, putamen, substantia nigra, subthalamic nucleus, and thalamus, bilaterally, which we also detected in both datasets using NEDICA on Z data. A reason that would explain why NEDICA failed to differentiate these subsections is that the signal in a subregion of the striatum and the thalamus may be made up of two components: one fairly homogeneous component within the entirety of the structure and another component more specific to the function subserved by this subregion. The fact that a single component comprising mainly the caudate nucleus, the putamen, and a large section of the thalamus was extracted from Z data suggests that the signal within these structures is specific and synchronous within these regions, but different from the signal detected in the other cortical regions. This subcortical component would explain why part of the dynamics within the striatum and the thalamus is homogeneous. The GLM proposed in this work segregates the striatum and the thalamus into several subregions, whose signal is closely linked to the average signal corresponding with the different functional networks. This suggests that within the striatum and the thalamus some features of the signal are specific to the function carried out by their subregions.

An intuitive idea would have been to apply sICA directly on the striatum and the thalamus extracted from the rest of the brain to identify the SC of the functional networks. For instance, Kim and coworkers (2013) applied a group ICA on a volume of interest comprising subcortical regions.

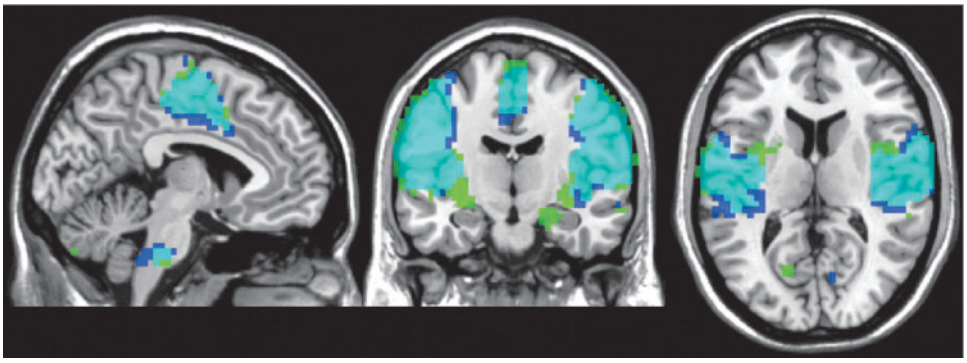

FIG. 3. MOT networks obtained from Z (in green) and Z_C (in dark blue), and their overlap (in cyan), superimposed on an anatomical template from the MNI.

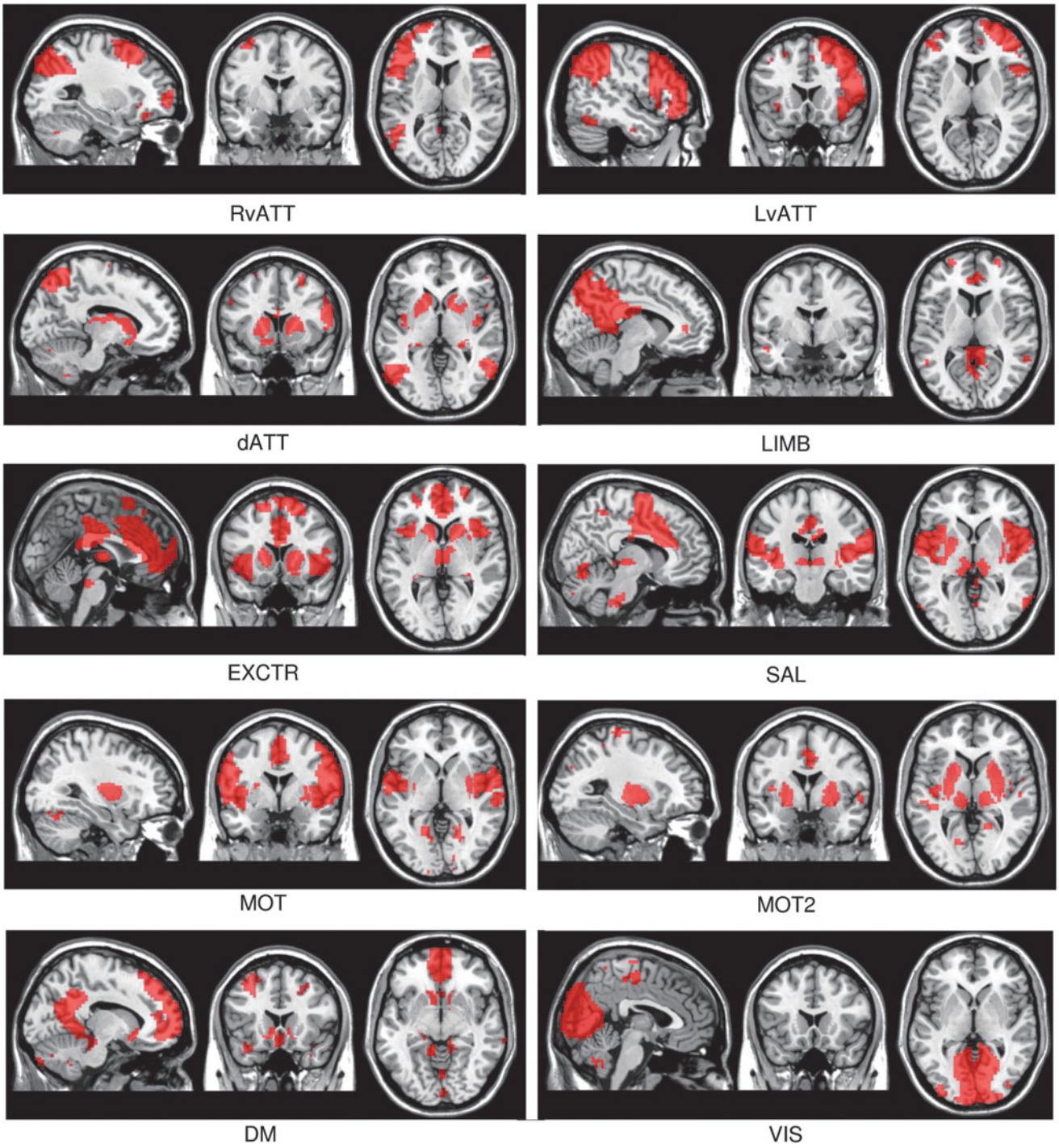

FIG. 4. Networks obtained with the proposed method (cortical and subcortical components [SC] in red) superimposed on an anatomical template.

However, such a method should be taken with caution, because sICA requires the presence of noise in the data, whether physiological (cardiac or respiratory) or not, to detect reproducible spatial components. In fact, for NEDICA to extract these independent spatial components, the type of noise present in the striatum and the thalamus should be similar to that in cortical areas. The areas most often studied for noise components are the CSF, the white matter, the outline of the brain, and so on. Therefore, it is necessary to include these structures when extracting the components. Cordes and Nandy (2007), indeed, demonstrated that the addition of noise in sICA model increased the accuracy of the mixing matrix by 5% and, as a result, the accuracy of the spatial sources. The alternative could have been to apply sICA on a dataset where only the cortical ribbon would be masked, hence containing subcortical gray matter, white matter, and CSF. However, we suspect that the proportion of gray matter would have been low compared with that of white matter and

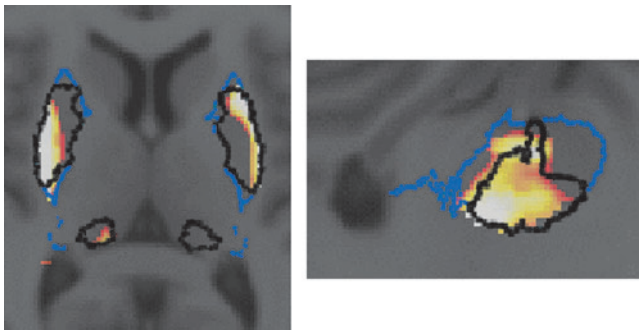

FIG. 5. Comparison between SC obtained using the proposed method and the postmortem atlas. Axial view (left) and sagittal view (right) of the SC for the MOT network (color scale from red to white), superimposed on the postmortem atlas. The atlas segmentation for the motor territory of the putamen and pulvinar is outlined in black; the outline of the entire putamen is shown in blue.

CSF, therefore preventing sICA from separating gray matter subcortical regions into individual components. On the other hand, if sICA had succeeded in segregating individual SC, this would not have solved the issue of matching these components to cortical functional networks. We still would have needed a functional criterion to associate striatal and thalamic regions to the cortical areas and this would have led us anyway to assume time course similarity.

Kim and associates (2013) addressed this issue by computing a functional connectivity index (namely, the correlation) between cortical IC from a group ICA conducted on the whole brain, and subcortical IC from a separate group ICA conducted on subcortical regions, looking for significant correlations between pairs of IC time series. This approach is similar to connectivity analyses based on regions of interest. By contrast, we proposed to use a GLM to parcellate the striatum and the thalamus into different subregions that can directly be associated with the different cortical networks. Indeed, the GLM tries to determine the subcortical voxels whose measured time course is closely related with the average time course of the cortical networks. The cortical information is taken into account in the GLM through the choice of regressors, which are nothing but the average signals in cortical regions for each functional network. The proposed procedure is a mixed-effect statistical analysis, including a first-level individual GLM accounting for within-subject variance and a second-level group analysis accounting for between-subject variance, using bootstrap-based inference to ensure robustness of the regions at the group level.

The method presented in this article enables voxels in the striatum and the thalamus to be segmented according to their functional links with the voxels in the cortex and classified into regions belonging to different functional networks. This has been visually and quantitatively validated with two datasets, thanks, in particular, to the use of an immunohistochemical functional atlas (Bardinet et al., 2009; Yelnik et al., 2007). We showed good consistency between SC detected in the striatum and the thalamus and functional territories from the atlas. Furthermore, within the striatum and the thalamus, the regions obtained for a given cortical network overlapped by at least 69% between both analysed datasets. The atlas also played a vital role in classifying the subcortical regions for each functional network, leading to the determination of functional belonging for these regions. We found that sensorimotor territories were mainly present in the motor functional networks, and associative sections from the atlas were found mainly in the right and left attentional ventral and attentional dorsal networks; limbic sections from the atlas were found mainly in the default mode network and the executive control network. In particular, for the default mode network, the subcortical regions that were detected included the associative and limbic caudate nucleus, the limbic putamen, and several (ventro-lateral and medio-dorsal) thalamic nuclei. These regions with limbic dominance are in agreement with the literature. For the VIS, the functional territories of the atlas were not involved, which may seem surprising as some thalamic structures (namely the lateral geniculate nucleus [LGN], the pulvinar, and the reticular peri-thalamic nucleus [Trpt, also known as the thalamic reticular nucleus]) are known to be involved in visual function (Saalmann and Kastner, 2011). Indeed, the LGN sends inputs to the primary visual cortex V1; however, this very small structure was not referenced in the immunohistochemical atlas, and hence was not present in the subcortical mask used in our procedure. This explains why we did not find any overlap between the SC of VIS and the atlas. ''Top-down'' inputs from V1 to the Trpt have also been suggested to be a consequence of attentional activation in V1 (Montero, 2000); however, our study was based on resting-state data with eyes closed and no external stimulus, and this may explain why no implication of this structure was found. On the other hand, we found that the pulvinar and the Trpt were involved for instance in the dorsal and ventral attentional networks, which contained associative visual regions.

Besides, it should be noted that the functional networks extracted did not belong exclusively to one functional category, sensorimotor, associative, or limbic. Indeed, in most cases, they belonged to two categories with a dominant component. For example, the motor network MOT2 mainly overlapped not only the sensorimotor putamen but also the associative putamen. Similarly, the default mode network overlapped not only limbic regions (limbic caudate nucleus and limbic putamen), but also the associative (medio-dorsal) thalamus and the caudate nucleus. This demonstrates that the functional networks identified cannot be considered purely associative, limbic, or sensorimotor, but rather, they result from a set of cognitive functions interacting with one another, through common regions.

The results also show that the striatum was highly involved in all functional networks. This finding conforms to other studies, which indicate that the striatum receives projections from the entire cortex (Alexander et al., 1986; Gopinath et al., 2011). This implies that this subcortical region has many connections with the sensorimotor cortex as well as with associative and limbic cortices.

Furthermore, the fact that results from both datasets were similar for the majority of functional networks (at least 69% subcortical overlap between the two datasets, and non-significant KS tests when comparing the datasets network by network, hemisphere by hemisphere) demonstrates the robustness of the method put forward in this work.

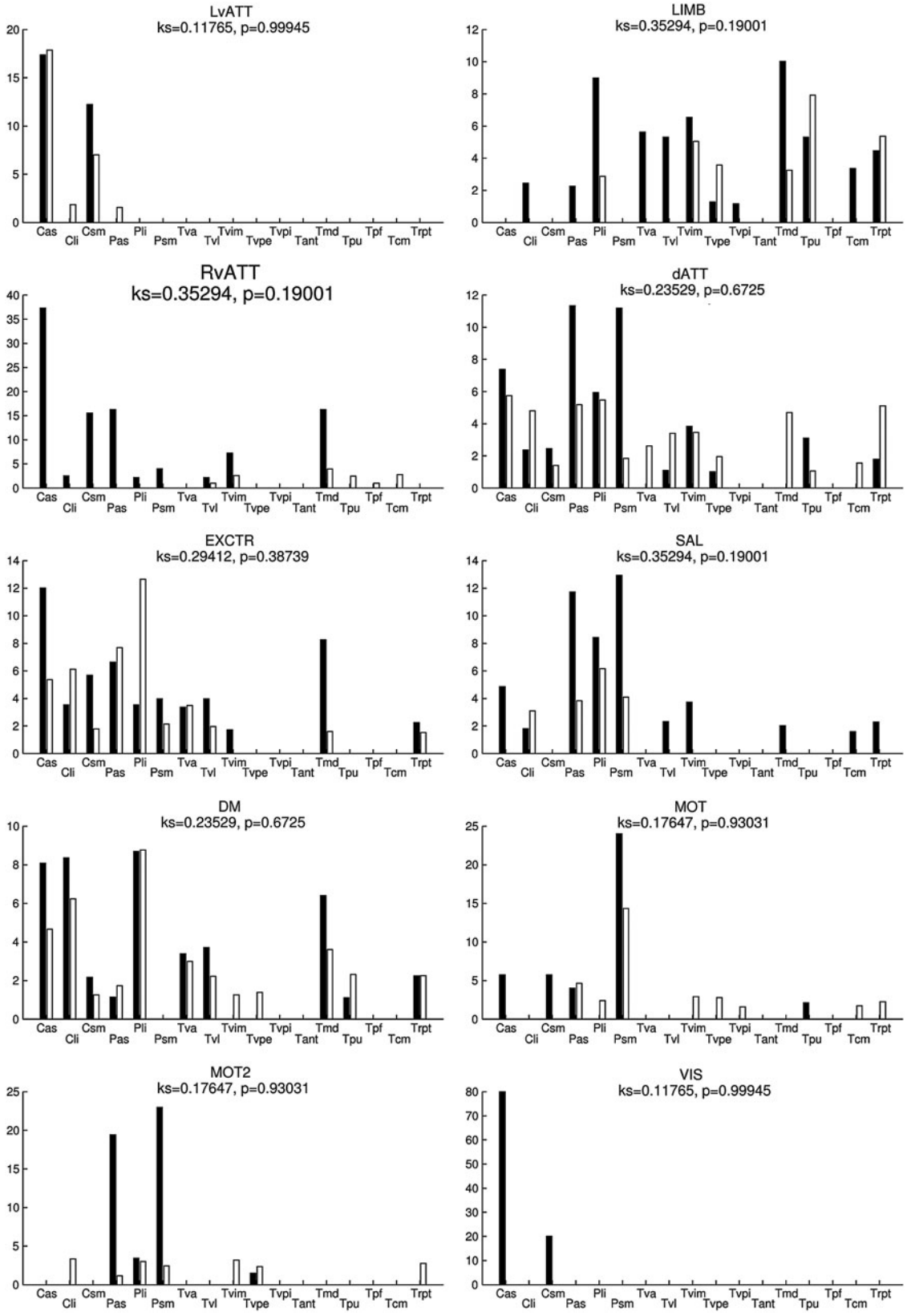

FIG. 6. Percentage of voxels (V_{comp}) of the SC maps (thresholded at $p < 0.01$, uncorrected) in each subcortical functional territory (SFT) of the atlas for each functional network, for the right hemisphere. The results from dataset 1 (resp. dataset 2) are shown in black (resp. white). The structures examined included the caudate nucleus (C) and the putamen (P) and their respective associative (as), limbic (li), and sensorimotor (sm) territories, and the thalamus (T) with the anterior ventral (va), ventrolateral (vl), intermediary ventral (vim), ventral posterior external and internal (vpe and vpi, respectively), anterior (ant), mediodorsal (md), parafascicular (pf), and centromedian (cm) parts, the pulvinar (pu), and the reticular peri-thalamic nucleus (rpt).

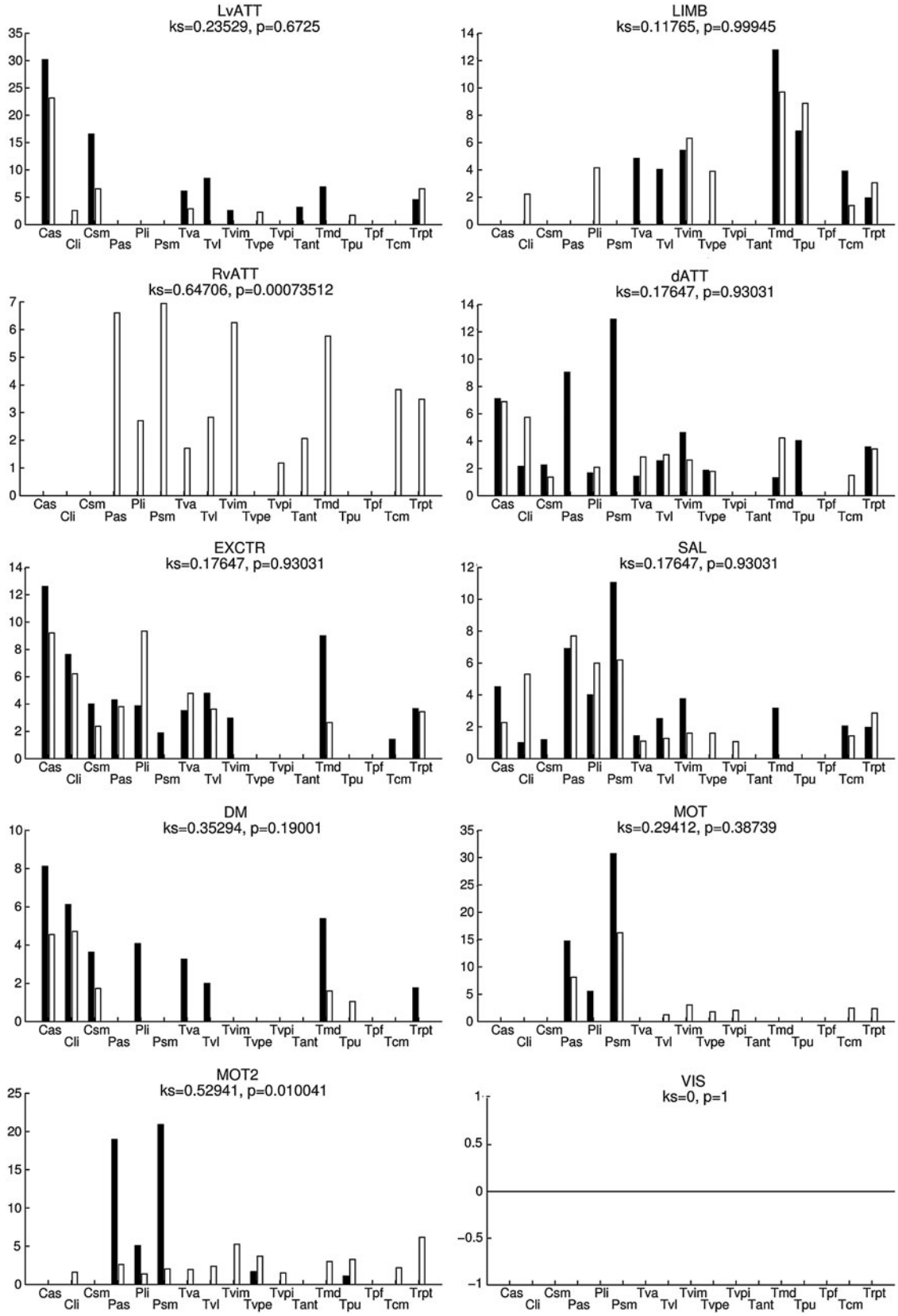

FIG. 7. Percentage of voxels (V_{comp}) of the SC maps (thresholded at $p < 0.01$, uncorrected) in each SFT of the atlas for each functional network, for the left hemisphere. See Figure 6 for notations.

Table 2. Relative Overlap of Subcortical Components Obtained from the Two Datasets, for Each Functional Network, with Group Maps Thresholded at $p < 0.01$, Uncorrected

Label	*Overlap (%)*
LvATT	0.8949
RvATT	0.9909
dATT	0.7323
LIMB	0.6908
EXCTR	0.7140
SAL	0.7564
MOT	0.7819
MOT2	0.8130
DM	0.9414
VIS	0.9897

The most important limitation that we can raise about the method is related to the actual lack of independence in spatial components extracted by sICA. Indeed, Daubechies and colleagues (2009) highlighted that algorithms such as InfoMax and FastICA accurately capture spatial variability in activity patterns, but these algorithms are barely selective for independence. Moreover, they showed that the components were more sparse than independent. Another limitation comes from the low threshold used to compare datasets and SFT. Due to possible normalization inaccuracy in the striatum and the thalamus, and since the studied SFT are really close to one another, the detection of accurate SC is far from easy. If we chose a higher threshold, the overlaps between the two datasets would be less significant. Moreover, the lack of independence of individual spatial components may hinder the detection of accurate SC with a high threshold, across many datasets.

Later on, it would be interesting to study cortico-subcortical interaction using diffusion MRI (dMRI). Indeed, dMRI enables noninvasive access to cortico-subcortical loops, by tracking white matter fibers. It can be used alone (Draganski et al., 2008; Lehéricy et al., 2004) or combined with fMRI (Johansen-Berg et al., 2005). Behrens and coworkers (2003) segregated the thalamus using anatomical connections obtained by probabilistic tractography between the thalamus and the cortex. We plan to compare their segregation with the results obtained with the proposed method.

Another aspect of the study would be to compare results obtained from healthy subjects with those from patients suffering from pathologies associated with a documented dysfunction of cortico-subcortical loops.

Conclusion

We have proposed a mathematical data-driven method that, for the first time, provided access to both cortical and subcortical components of functional networks using resting-state fMRI. The proposed method accurately identified cortico-subcortical functional networks, as shown by the agreement between these networks and well-known anatomical and functional cortico-subcortical networks. The similarity of the results obtained from two different datasets further demonstrated the robustness of the method.

Acknowledgments

The authors are grateful to the Centre de Recherche de l'Institut Universitaire de Gériatrie de Montréal, Montréal QC, Canada, for providing data for this work. They are also very grateful to A. Villringer for making his data freely available on the 1000 Functional Connectomes Project website. C.M. was funded by the French National Agency for Research (ANR 07 NEURO 023-01).

Author Disclosure Statement

No competing financial interests exist.

References

Alexander GE, DeLong MR, Strick PL. 1986. Parallel organization of functionally segregated circuits linking basal ganglia and cortex. Annu Rev Neurosci 9:357–381.

Bardinet E, Bhattacharjee M, Dormont D, Pidoux B, Malandain G, Schüpbach M, et al. 2009. A three-dimensional histological atlas of the human basal ganglia. II. Atlas deformation strategy and evaluation in deep brain stimulation for Parkinson disease. J Neurosurg 110:208–219.

Beckmann CF, DeLuca M, Delvin JT, Smith SM. 2005. Investigations into resting-state connectivity using independent component analysis. Philos Trans R Soc Lond B Biol Sci 360:1001–1013.

Behrens TE, Johansen-Berg H, Woolrich MW, Smith SM, Wheeler-Kingshott CA, Boulby PA, et al. 2003. Noninvasive mapping of connections between human thalamus and cortex using diffusion imaging. Nat Neurosci 6:750–757.

Biswal BB, Mennes M, Zuo XN, Gohel S, Kelly C, Smith SM, et al. 2010. Toward discovery science of human brain function. Proc Natl Acad Sci U S A 107:4734–4739.

Biswal BB, Yetkin FZ, Haughton VM, Hyde JS. 1995. Functional connectivity in the motor cortex of resting human brain using echo-planar MRI. Magn Reson Med 34:537–541.

Cordes D, Nandy R. 2007. Independent component analysis in the presence of noise in fMRI. Magn Reson Imaging 25:1237–1248.

Damoiseaux JS, Beckmann CF, Arigita EJ, Barkhof F, Scheltens P, Stam CJ, et al. 2008. Reduced resting-state brain activity in the ''default network'' in normal aging. Cereb Cortex 18:1856–1864.

Damoiseaux JS, Rombouts SARB, Barkhof F, Scheltens P, Stam CJ, Smith SM, et al. 2006. Consistent resting-state networks across healthy subjects. Proc Natl Acad Sci U S A 103: 13848–13853.

Daubechies I, Roussos E, Takerkart S, Benharrosh M, Golden C, D'Ardenne K, et al. 2009. Independent component analysis for brain fMRI does not select for independence. Proc Natl Acad Sci U S A 106:10415–10422.

Draganski B, Kherif F, Klöppel S, Cook PA, Alexander DC, Parker GJM., et al. 2008. Evidence for segregated and integrative connectivity patterns in the human basal ganglia. J Neurosci 28:7143–7152.

Efron B, Tibshirani RJ. 1993. *An Introduction to the Bootstrap*. New York: Chapman & Hall.

Fox MD, Raichle ME. 2007. Spontaneous fluctuations in brain activity observed with functional magnetic resonance imaging. Nat Rev Neurosci 8:700–711.

Genovese CR, Lazar NA, Nichols TE. 2002. Thresholding of statistical maps in functional neuroimaging using the false discovery rate. Neuroimage 15:870–878.

Gopinath K, Ringe W, Goyal A, Carter K, Dinse HR, Haley R, et al. 2011. Striatal functional connectivity networks are modulated by fMRI resting state conditions. Neuroimage 54:380–388.

Habas C, Kamdar N, Nguyen D, Prater K, Beckmann CF, Menon V, et al. 2009. Distinct cerebellar contributions to intrinsic connectivity networks. J Neurosci 29:8586–8594.

Hartigan JA. 1975. *Clustering Algorithms*. New York: John Wiley and Sons.

Johansen-Berg H, Behrens TE, Sillery E, Ciccarelli O, Thompson AJ, Smith SM, et al. 2005. Functional-anatomical validation and individual variation of diffusion tractography-based segmentation of the human thalamus. Cereb Cortex 15:31–39.

Kim DJ, Park B, Park HJ. 2013. Functional connectivity-based identification of subdivisions of the basal ganglia and thalamus using multilevel independent component analysis of resting state fMRI. Hum Brain Mapp 34:1371–1385.

Lehéricy S, Ducros M, Van de Moortele PF, Francois C, Thivard L, Poupon C, et al. 2004. Diffusion tensor fiber tracking shows distinct corticostriatal circuits in humans. Ann Neurol 55:522–529.

Montero VM. 2000. Attentional activation of the visual thalamic reticular nucleus depends on 'top-down' inputs from the primary visual cortex via corticogeniculate pathways. Brain Res 864:95–104.

Parent A, Sato F, Wu Y, Gauthier J, Lévesque M, Parent M. 2000. Organization of the basal ganglia: the importance of axonal collateralization. Trends Neurosci 23:S20–S27.

Perlbarg V, Marrelec G, Doyon J, Pélégrini-Issac M, Lehéricy S, Benali H. NEDICA: Detection of Group Functional Networks in fMRI Using Spatial Independent Component Analysis. In Proceedings of the IEEE International Symposium on Biomedical Imaging: From Nano to Macro (ISBI'08), Paris, France, 2008.

Purves D, Augustine GJ, Fitzpatrick D, Hall WC, LaMantia AS, McNamara JO. 2004. *Neuroscience*. Sunderland: Sinauer Associates, Inc.

Robinson S, Basso G, Soldati N, Sailer U, Jovicich J, Bruzzone L, et al. 2009. A resting-state network in the motor control circuit of the basal ganglia. BMC Neurosci 10:137.

Saalmann YB, Kastner S. 2011. Cognitive and perceptual functions of the visual thalamus. Neuron 71:209–223.

Smith SM, Fox PT, Miller KL, Glahn DC, Fox PM, Mackay CE, et al. 2009. Correspondence of the brain's functional architecture during activation and rest. Proc Natl Acad Sci U S A 106:13040–13045.

Smith Y, Raju DV, Pare JF, Sidibe M. 2004. The thalamostriatal system: a highly specific network of the basal ganglia circuitry. Trends Neurosci 27:520–527.

Varela FJ, Lachaux JP, Rodriguez E, Martinerie J. 2001. The brainweb: phase synchronization and large-scale integration. Nat Rev Neurosci 2:229–239.

Worsley KJ, Liao CH, Aston J, Petre V, Duncan GH, Morales F, et al. 2002. A general statistical analysis for fMRI data. Neuroimage 15:1–15.

Yelnik J, Bardinet E, Dormont D, Malandain G, Ourselin S, Tandé D, et al. 2007. A three-dimensional, histological and deformable atlas of the human basal ganglia. I. Atlas construction on immunohistochemical and MRI data. Neuroimage 34:618–638.

Zhang D, Snyder AZ, Fox MD, Sansbury MW, Shimony JS, Raichle ME. 2008. Intrinsic functional relations between human cerebral cortex and thalamus. J Neurophysiol 100: 1740–1748.

Address correspondence to:
Mélanie Pélégrini-Issac
LIB —Laboratoire d'Imagerie Biomédicale
Sorbonne Universités, UPMC Univ Paris 06
Inserm UMR_S 1146- CNRS UMR 7371
91 bd de l'Hôpital
F-75634 Paris Cedex 13
France

E-mail: melanie.pelegrini@imed.jussieu.fr

Appendix

Appendix A

This appendix describes the automatic iterative procedure used to merge all the independent components into classes that are the most representative of the population. Ideally, each class should contain one and only one independent component (IC) from each subject. Thus, from the similarity tree (the so-called dendrogram) that describes IC clustering as a function of within-class spatial similarity, group-representative classes are chosen so as to optimize both the degree of representativity (DR) and the degree of unicity (DU) of each class. For a given class, DR is defined as the number of subjects N_s that contribute to the class, divided by the total number of subjects. Since a subject may contribute to a class with more than one IC, DU is defined as the number of subjects that contribute to the class with one and only one IC, divided by N_s. An optimal class would then be characterized by $DR = 1$ and $DU = 1$. In our procedures, we set score limits to $DR > 0.5$ and $DU > 0.75$, that is, for each class, at least half of the subjects contribute to the class and at least 75% of these subjects contribute with only one IC. When both conditions are not simultaneously fulfilled, DR is privileged over DU. For instance, consider a class B with $DR(B) > 0.5$ but $DU(B) < 0.75$, obtained by merging two classes A_1 and A_2 with $DR(A_1) < 0.5$ and $DR(A_2) < 0.5$. The procedure retains class B rather than the separate classes A_1 and A_2. The algorithm ends when all IC are assigned to a class. The final number of classes is not predefined.